In vivo single-molecule detection of nanoparticles for multiphoton fluorescence correlation spectroscopy to quantify cerebral blood flow

Xu Fu†, Pradoldej Sompol‡, Jason A. Brandon§, Christopher M. Norris‡, Thomas Wilkop¶, Lance A. Johnson‡, §, and Christopher I. Richards†**

†. Department of Chemistry, University of Kentucky, Lexington, KY 40506

‡. Sanders-Brown Center on Aging, University of Kentucky, Lexington, KY 40536

§. Department of Physiology, University of Kentucky, Lexington, KY 40536

¶. Light Microscopy Core, University of Kentucky, Lexington, KY 40536

*chris.richards@uky.edu and Johnson.Lance@uky.edu

Supplementary Methods

Animals

All experiments were conducted within the guidelines set forth by the National Institutes of Health (NIH) and were approved by the Institutional Animal Care and Use Committee (IACUC) at the University of Kentucky. The study used both female and male mice (C57BL/6) that were 3-6 months old. Mice were housed in cages in group of three or four animals before surgery and maintained with standard housing conditions until use.

Animal Preparation

All surgical procedures were conducted in a custom-made stereotaxic apparatus with temperature controlled (homeothermic pad). Briefly, mice were deeply anesthetized with isoflurane (3% for induction, 2.0% to 2.5% for surgery) and subjected to head-bar surgeries. After anesthesia induction, toe-pinch nociceptive reflex responses were tested. To obtain optical access, we created an open or non-open cranial window on both sides of mouse hemisphere (approximately 1 mm posterior and 1 mm lateral from bregma). In the preparation of the thin-skull window, the scalp was removed, and the surface of the skull, around 5 mm diameter circular area, was polished with a dental drilling tool until the bone reached transparent to see vasculature. We applied GenTeal lubricant eye gel to cover the thinned skull surface to keep moisture. After the thin-skull surgery, the mouse was directly moved to microscope stage to continue the *in vivo* imaging. In the open skull cranial window surgery, the scalp was removed, and the surface of the skull was gently scraped to increase adherence of the head holder. The cranial window was filled with saline after a 3 mm diameter skull bone was lifted, and a 5 mm circular coverglass (#1 thickness) was covered and secured with cyanoacrylate glue (Loctite 416). We then spread the glue over the skull up to the edge of the skin and cemented a 3D printed head holder to the skull using dental cement for head fixation during imaging. After the craniotomy surgery, the mouse was returned to its home cage and allowed to recover for several days before imaging sessions.

Multiphoton FCS setup

Fluorescence correlation spectroscopy was performed with a commercial upright confocal microscope (LSM 880 laser scanning microscope, Carl Zeiss, Germany), equipped with an InSight

X3 wavelength tunable (680 to 1300 nm) infrared laser. Imaging and FCS recordings were carried out with a long working distance water immersion objective (W Plan-Apochromat 20x/1.0, Carl Zeiss). The choice of objective is an important consideration as it is the primary determining factor in the spatial resolution of this method. A long working distance is required for depth of penetration while a high numerical aperture for higher resolution. This objective was chosen to allow for imaging deep into the brain while maintaining a sub-micron spatial resolution. Fluorescence emission was directed with a long pass dichroic mirror onto two non descanned GaAsP detectors mounted to the side of microscope nosepiece and bandpass filters matching the emission of each fluorophore were mounted in front of the detectors. Zeiss ZEN Black 2.3, with the advanced FCS module was used for recording the images and the time correlated single photon counting (TCSPC) data for the FCS measurements. The same software was used for analyzing and fitting the FCS data.

Microfluidic chamber flow measurements

A microfluidic chamber was used to determine the appropriate fluorescence dye and to calibrate the focal diameter of the system. Briefly, a syringe pump was connected by a tube to a glass coverslip covered microchannel (Ibidi, Germany) to control the flow rate[1] (Supplementary Fig. S2). The flow volume was set to a series of values ranging from 0.3 mL/min to 1.5 mL/min. The dimensions (0.1 x 5 x 48.2 mm) of the chamber are shown in the Figure 1. After these initial measurements, we tested several fluorophores for multiphoton FCS measurements (Supplementary Fig. S2). All fluorescent probes were dissolved in MilliQ water and diluted to a concentration that yielded approximately 5 molecules in the focal volume. We compared the brightness and stability of all the fluorescent dyes. Of the brightest fluorophores, we selected two fluorescent dyes with well separated 2-photon excitation wavelengths to minimize crosstalk during signal collection. The excitation wavelength of the vessel labeling dye (high concentration dye) was selected for its shorter excitation wavelength and FCS indicator dye (low concentration dye) for its longer excitation wavelength. CF488-dextran 250 kDa was chosen as the FCS dye (920 nm excitation) and Rhodamine B-dextran 500 kDa as the vessel labeling dye (820 nm excitation). CF 488 and Rhodamine B were selected or *in vivo* measurements. CF488 Dextran 250 kDa was purchased from Biotium, and Rhodamine B Dextran 500 kDa was purchased from Nanocs. To diminish bias and accurately calibrate the system, a short acquisition time with multiple repetitions

(e.g., 10 reps x 10 s) was used in the presence and absence of flow. Averaging of short acquisitions can help recognize the extraordinary events such as inadvertent spikes due to dust or other anomalies such as breathing artifacts and these can then be excluded from the final data analysis[2]. The autocorrelation function was further fitted in ZEN Black 2.3 software (Carl Zeiss, Germany) with following equation (Equation 4):

$$G(\tau) = \frac{1}{<N>}\left[1 + \frac{T_t}{1-T_t}\exp\left(-\frac{\tau}{\tau_t}\right)\right]\frac{1}{\left[1+\frac{\tau}{\tau_d}\right]\sqrt{1+\frac{\tau}{S^2\tau_d}}} \qquad (4)$$

Here, N is the total number of fluorescence particles in the focal volume, T_t is the triplet fraction, and τ_t is the triplet decay time (the lifetime of the dark state). τ_d is the diffusion time and S is the structure parameter which is defined as the ratio between axial and lateral dimensions of the focal volume. This fitting model allows us to extract the free diffusion time of pure fluorescence species from FCS curves. In the presence of flow, the residence time (τ_f) can be extracted by fitting the autocorrelation function G(τ) to equations 1 and 2. The lateral diameter of detection volume (d) is linked to the velocity (υ) by $d = \tau_f * \upsilon$. Thus, to calibrate the focal volume of our system with CF488 dextran 250kDa, we examined a series of flow rates to extract the residence time. In addition, we have also tested CF488 dextran 10kDa to further examine and calibrate the focal detection volume. The equatorial diameter of the focal volume with CF488-dextran 10 kDa and CF488-dextran 250 kDa was calculated to be 0.87 μm and 0.98 μm, respectively. Details of the focal volume calibration can be found in Supplementary Fig. S1, and Supplementary Table 1 and 2.

***In vivo* imaging sessions**

During imaging sessions, mice were anesthetized with isoflurane (1.3% to 2.2% in O_2) and the body temperature was maintained with an electric heating pad under the mouse. To visualize the vasculature and measure the flow rate, 100 μL mixture of fluorescent dye (8 μM Rhodamine B Dextran 500 kDa and 300 nM CF488 Dextran 250kDa) was intravenously injected into a ~25 g mouse through either the tail vein or via retro-orbital injection. The final concentration in the animal was 20 nM for the FCS tracker and 530 nM for the vascular label. Similar to the FCS measurements in the microfluidic chamber, a short acquisition time with multiple repetitions (e.g., 6 reps x 5 s) was performed. The mouse head needed to be secured and stabilized to avoid breathing motion artifacts during the recording of FCS signals. Without sufficient immobilization, movement

during respiration led to artifacts in the fluorescence time trace. The background autofluorescence in the brain tissue was higher than that inside the vessel. Thus, an increase in intensity was observed when movement caused the excitation beam to be focused into the brain tissue and a return to baseline fluorescence when the animal relaxed and the beam realigned to the vessel. This was also observed in the subsequent autocorrelations, which showed components on the same time scale as the animal breathing. The effects of breathing artifacts on the photon counting were detailed in Supplementary Fig. S10. Thus, we designed and 3-D printed a custom mouse head holder, which minimized the movement of the anesthetized mouse, and ensured the contribution of fluorescence fluctuation from flow is much larger compared to fluctuations induced by breathing. After mounting the mouse's head in a custom-made head restraint under the microscope objective, we placed GenTeal lubricant eye gel between the window and the objective. The lubricant has the same index of refraction as water but has the advantage of a much higher viscosity and limited evaporation during long imaging sessions. Vessels approximately 100-200 μm deep in the neocortical tissue were selected for imaging.

To image the cerebral vasculature, we used the InSight X3 laser set to 820 nm to excite Rhodamine B. Two-Photon *in vivo* imaging was conducted to find large vessels and capillaries. We also performed multiphoton imaging to identify veins and arteries which were identified by tracing connections and determining whether they were surrounded by clear continuous lines of smooth muscle. Within the focal plane of a region of interest, we selected one (single pixel measurement) or several positions (pixel by pixel mapping) within different vessels. The scanned laser beam was positioned at our selected locations for the duration of the data collection. CF488 for FCS measurements was excited at 920 nm. Since exogenous fluorescent dyes are quickly cleared from the blood, all flow measurements were conducted within 60 min after injection. In order to maintain signal consistency during the flow measurements, we adjusted the amount of fluorescent dye injected according to the weight of the mice. The laser power was also adjusted to maintain a count rate of approximately 50 kHz during the FCS measurements. In addition, we have demonstrated the cy3 and rhodamine B pair also serves similarly as CF488 with rhodamine B pair, as shown in the Supplementary Fig. S11.

To map sub-vessel resolution blood flow velocity, we first positioned the laser beam in the center of the vessel of interest. Several positions across the entire vessel were selected in the same focal plane. Then the laser beam was moved sequentially to each position, and fluctuations in the fluorescence were collected in each coordinate. Similarly, to obtain the 2D sectional blood flow velocity profile, we found the center of the vessel and obtained the fluorescence intensity time trances and then relocated the measurement point 10 µm up and 10 µm down. For the dynamic flow studies, we slowly increased the isoflurane rate (from 1.3% to 2.2%) to decrease the animal's heart rate. Flow velocity was measured once the heart rate stabilized.

The flow velocity was calculated based on the earlier determined diameter of the detection volume according to Equation 5.

$$Flow\ velocity = \frac{lateral\ diameter}{residence\ time} \quad (5)$$

Supplementary Tables

Supplementary Table 1. Calibration of the focal volume through CF488-dextran 10 kDa

Flow rate (ml/min)	Area (mm^2)	Velocity (mm/s)	Residence time (µs)	Lateral diameter (µm)
0.1	0.5	3.33	265.595	0.885
0.2	0.5	6.67	131.253	0.875
0.3	0.5	10	87.416	0.874
0.4	0.5	13.33	63.831	0.851
0.5	0.5	16.67	52.862	0.881
0.6	0.5	20.00	43.007	0.860
0.7	0.5	23.33	36.252	0.846
0.8	0.5	26.67	32.02	0.854
0.9	0.5	30.00	29.02	0.871
1	0.5	33.33	26	0.867

Supplementary Table 2. Calibration of the focal volume through CF488-dextran 250 kDa

Flow rate (ml/min)	Area (mm^2)	Velocity (mm/s)	Residence time (μs)	Lateral diameter (μm)
0.3	0.5	10	97.6	0.976
0.4	0.5	13.33	73.4	0.979
0.5	0.5	16.67	62.0	1.032
0.6	0.5	20.00	49.7	0.994
0.7	0.5	23.33	42.7	0.996
0.8	0.5	26.67	36.7	0.980
0.9	0.5	30.00	32.6	0.980
1	0.5	33.33	29.4	0.980

Supplementary Figures

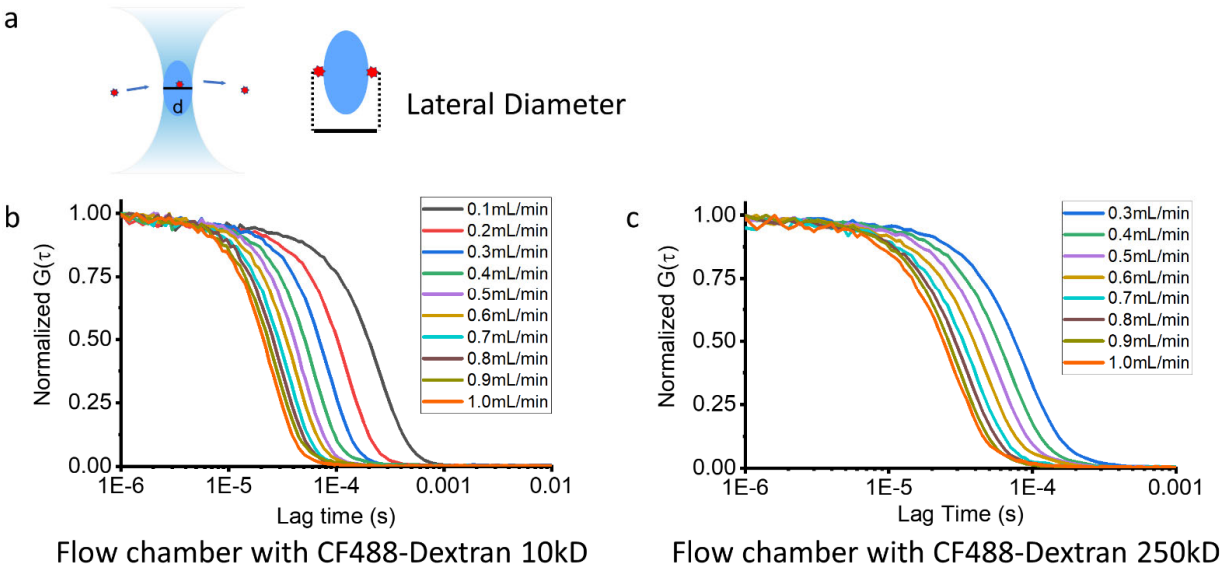

Figure S1: Calibration of FCS focal volume.

a. Schematic of FCS focal volume. **b** and **c**. Results of CF488-dextran 10 kDa and CF488-dextran 250 kDa normalized autocorrelations from bulk flow rates ranging from 0.1 mL/min to 1.0 mL/min.

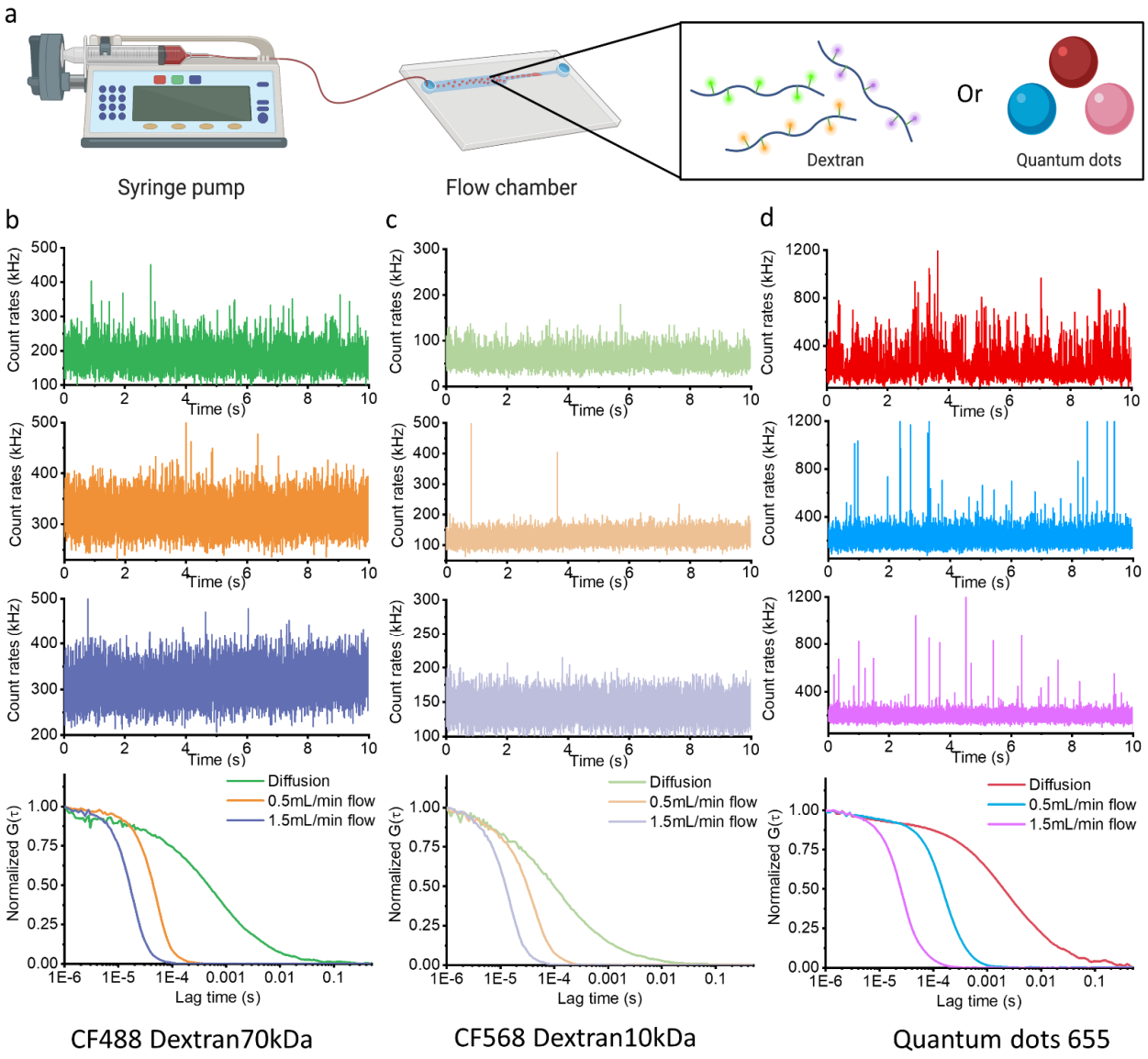

Figure S2: a. Schematic of the microfluidic chamber used to calibrate the optical setup. **b-d.** The recorded fluorescence fluctuations over time and their corresponding autocorrelation curves from CF488-dextran 70 kDa (**b**), CF568-dextran 10 kDa (**c**), and Quantum dots 655. (**d**). **b**, Photon counting time traces of CF488-dextran 70 kDa during free diffusion (upper panel, green), 0.5 mL/min flow rate (middle panel, orange), and 1.5 mL/min flow rate (lower panel, purple). **c**, Photon counting time traces of CF568-dextran 10 kDa at free diffusion (upper panel, light green), 0.5 mL/min flow rate (middle panel, light orange), and 1.5 mL/min flow rate (lower panel, light purple). **d**, Photon counting time traces of Quantum dots 655 at free diffusion (upper panel, red), 0.5 mL/min flow rate (middle panel, blue), and 1.5 mL/min flow rate (lower panel, pink).

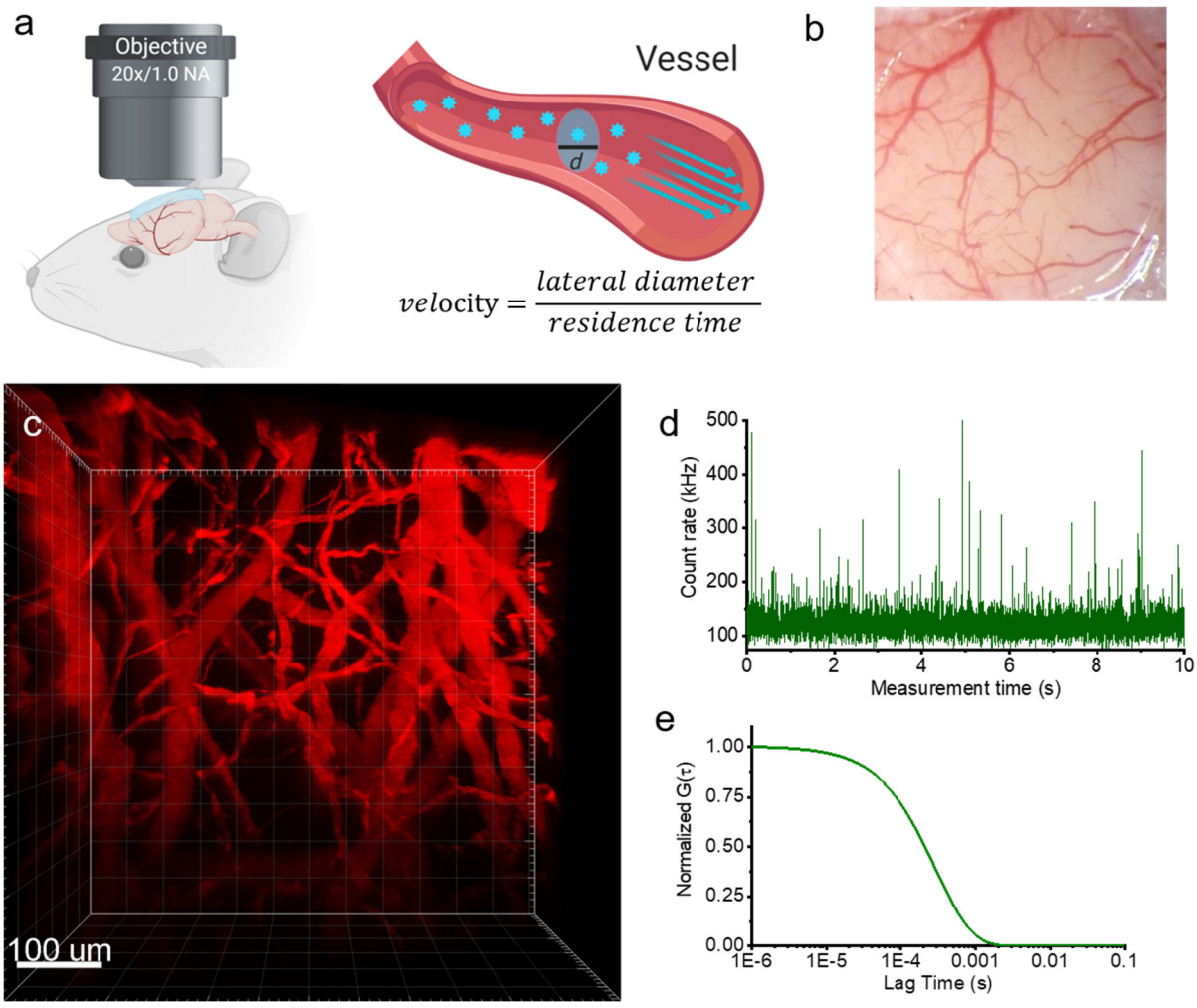

Figure S3: Illustration of the working principle of fluorescence correlation spectroscopy in two-photon *in vivo* microscopy.

a, Schematic of in vivo FCS measurements in blood vessels through a cranial window. The equation shows the simple relationship between blood flow velocity and FCS measured residence time. **b,** A representative 5mm thinned-skull window in a mouse hemisphere. **c,** A representative image of a 3-D reconstruction of blood vessels from in vivo 2P imaging. **d,** A fluorescence fluctuation time trace measured through a blood vessel *in vivo*. **e,** the corresponding ACF (G(τ)) reveals the fluorescent molecule flow residence time in the focal volume.

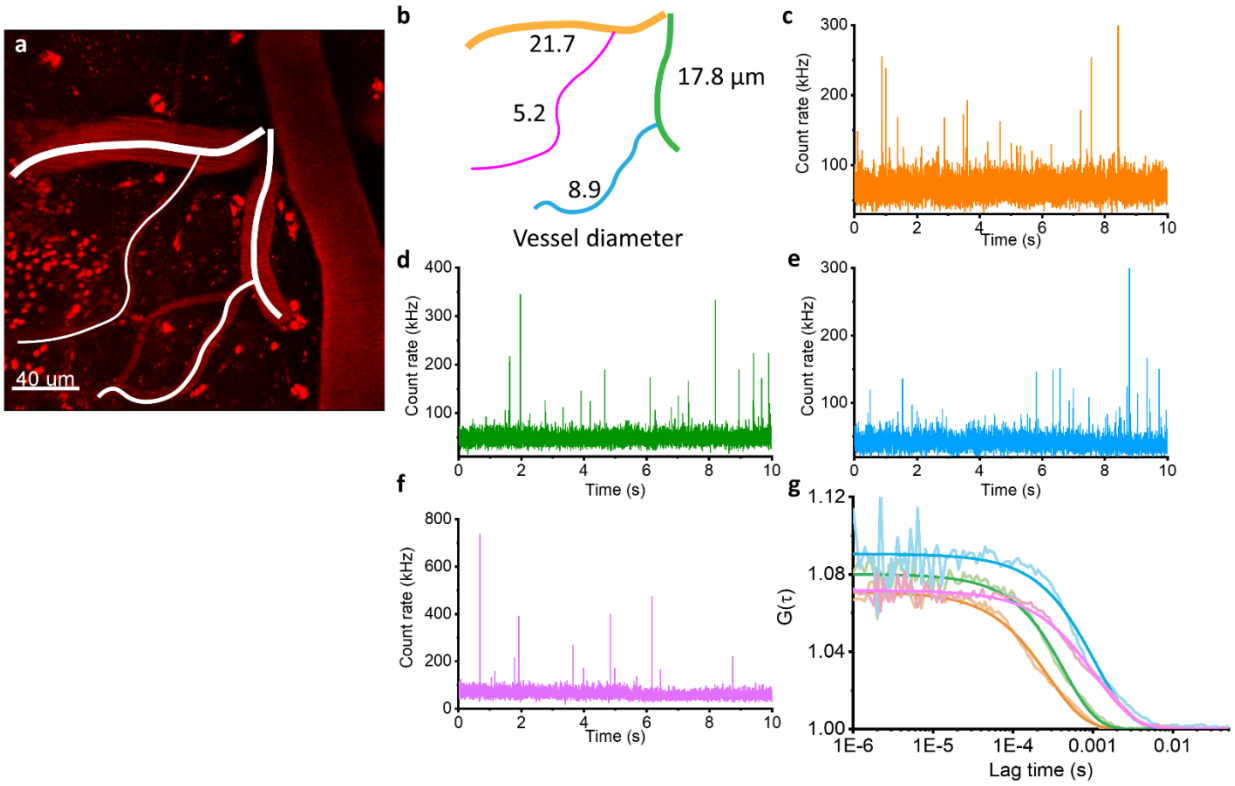

Figure S4: In vivo blood flow measurements of different sized vessels.

a. 2P-image of fluorescently labeled vasculature. **b.** Blood flow velocity measurements of the vascular network traced in (**a**). **c-f**. Fluorescence intensity time traces recorded from vessels traced in (**a** and **b**) with the corresponding color code. The orange panel: the center of 21.7 µm vessel; the green panel: the center of 17.8 µm vessel; the blue panel: 8.9 µm capillary; the pink panel: 5.2 µm capillary. **g.** The raw autocorrelations and their fits from the color matched time traces. The orange, green, blue, and pink curves give residence time of 362 µs, 515 µs, 1367 µs, and 1520 µs, respectively. Therefore, the calculated flow velocities are 2.7, 1.9, 0.72, and 0.65 mm/s, respectively.

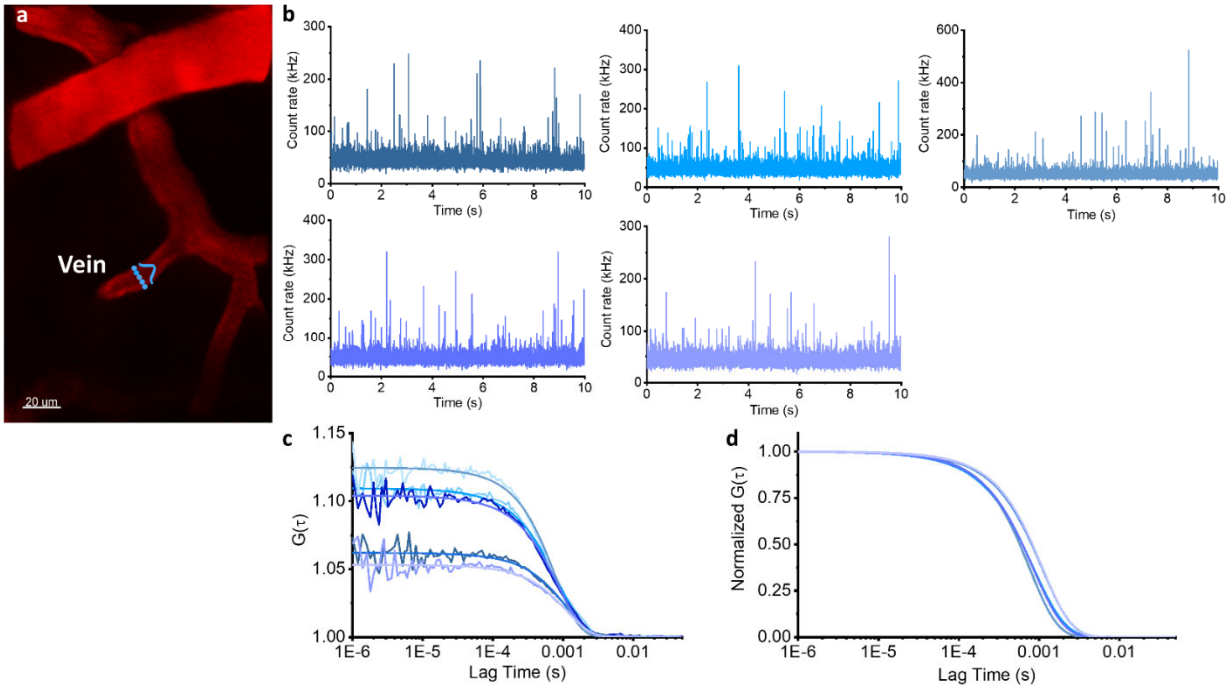

Figure S5: Blood flow velocity profiles across a vein.

a. 2P-image of fluorescently labeled vasculature. An apparent FCS cross section of flow velocity of a vein is generated by sequentially measuring across the vessel with the FCS detection spots indicated with blue circles. **b.** Fluorescence intensity time traces recorded at the opposite walls and then at increments across the vessel to build a flow velocity cross section. The scaled color from dark blue to light purple corresponded to the one side of the vein wall to the other side of the vessel wall. **c.** The measured and fit autocorrelation curves from color matched time traces. From the original curves, we noticed that blood flow through the center of vessel is larger than at the locations near the vessel wall. **d.** The normalized autocorrelation curves from **c**.

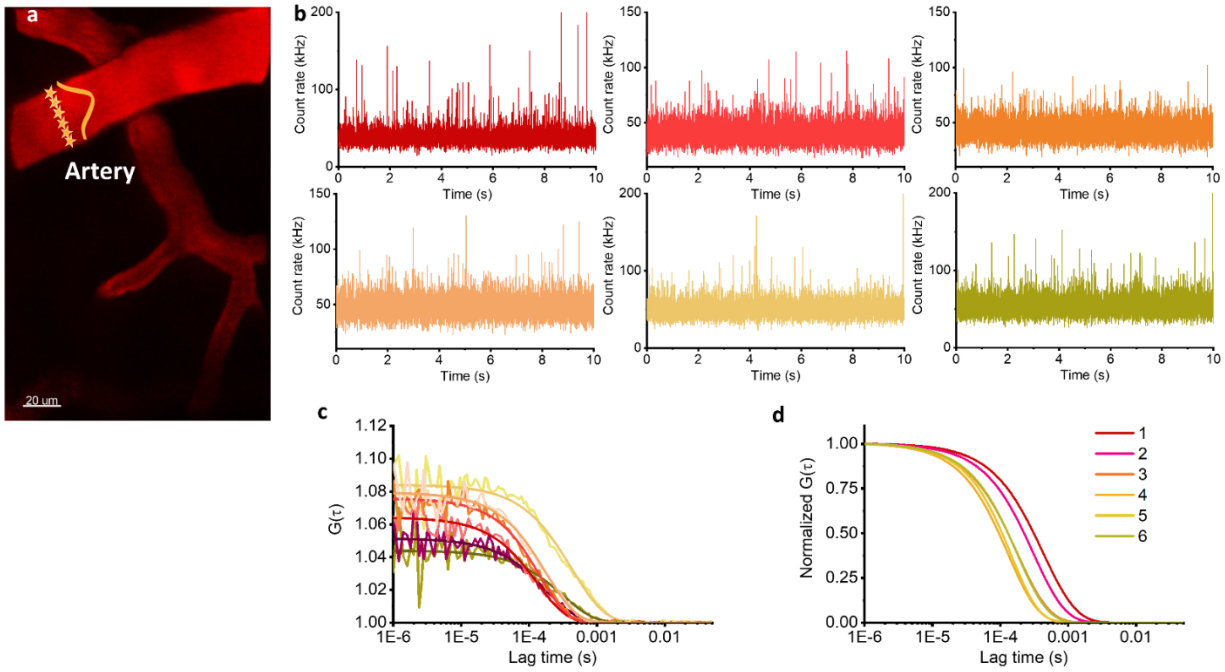

Figure S6: Blood flow velocity profiles across an artery.

a. 2P-image of fluorescently labeled vasculature. An FCS cross section of flow velocity of an artery is generated by sequentially measuring across the vessel with the FCS detection spots indicated with yellow starts. **b.** Fluorescence intensity time traces recorded at the opposite walls and then at increments across the vessel to build a flow velocity cross section. The scaled color from dark red to light green corresponded to the one side of the artery wall to the other side of the vessel wall. **c.** The measured and fitted autocorrelation curves from color matched time traces. **d.** The normalized the autocorrelation curves from **c**.

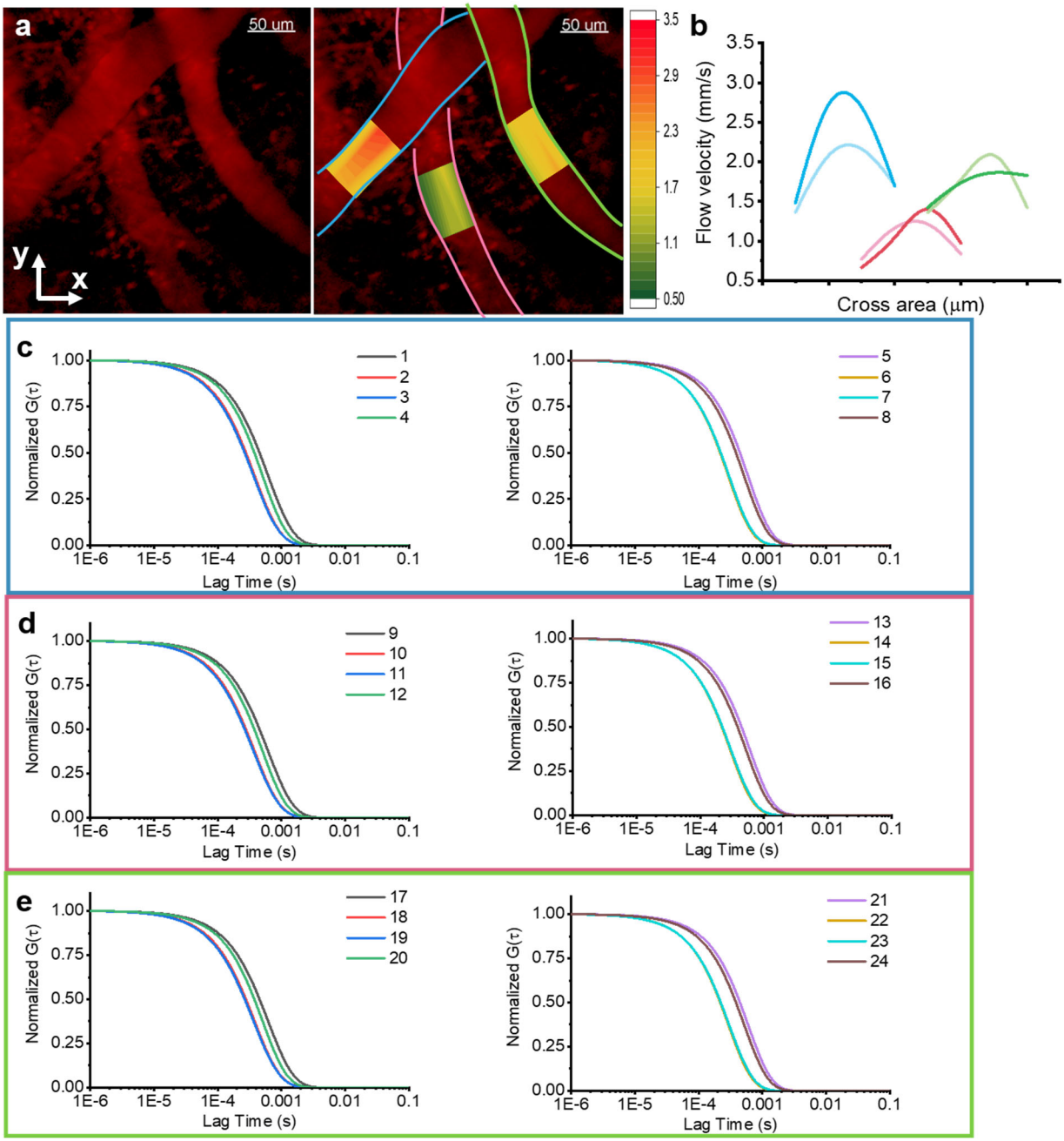

Figure S7: Mapping of blood flow rates.

a, A 2P image of a blood vessel from a 3 mm open cranial window and the corresponding flow velocity maps in three blood vessels (traced in blue, pink, and green color). The heat map corresponds to the flow velocity (see key: green to red, 0.5 mm/sec to 3.5 mm/sec). The central region of the vessel exhibits a higher velocity than the near the walls. **b**, The corresponding cross section blood flow velocity line profiles from **a**. **c-e.** The normalized autocorrelation curves show the flow velocity changes for 3 separate vessels, where **c**, **d**, **e** are for the blue, pink, and green line traced vessels, respectively.

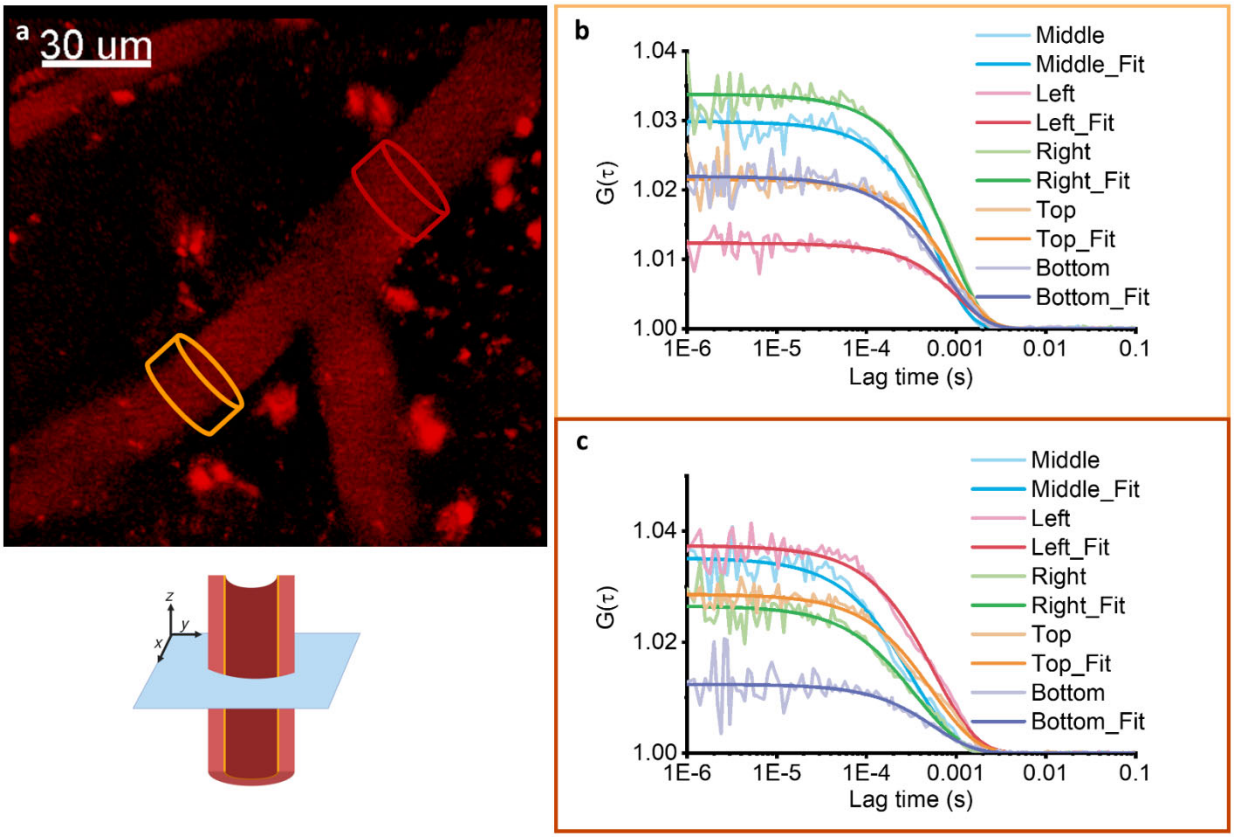

Figure S8: 2D cross-sectional blood flow measurements.

a. 2p image showing vessels measured at 2 locations to obtain the 2-D cross sectional flow. **b and c.** The recorded autocorrelation curves and fits from the two locations.

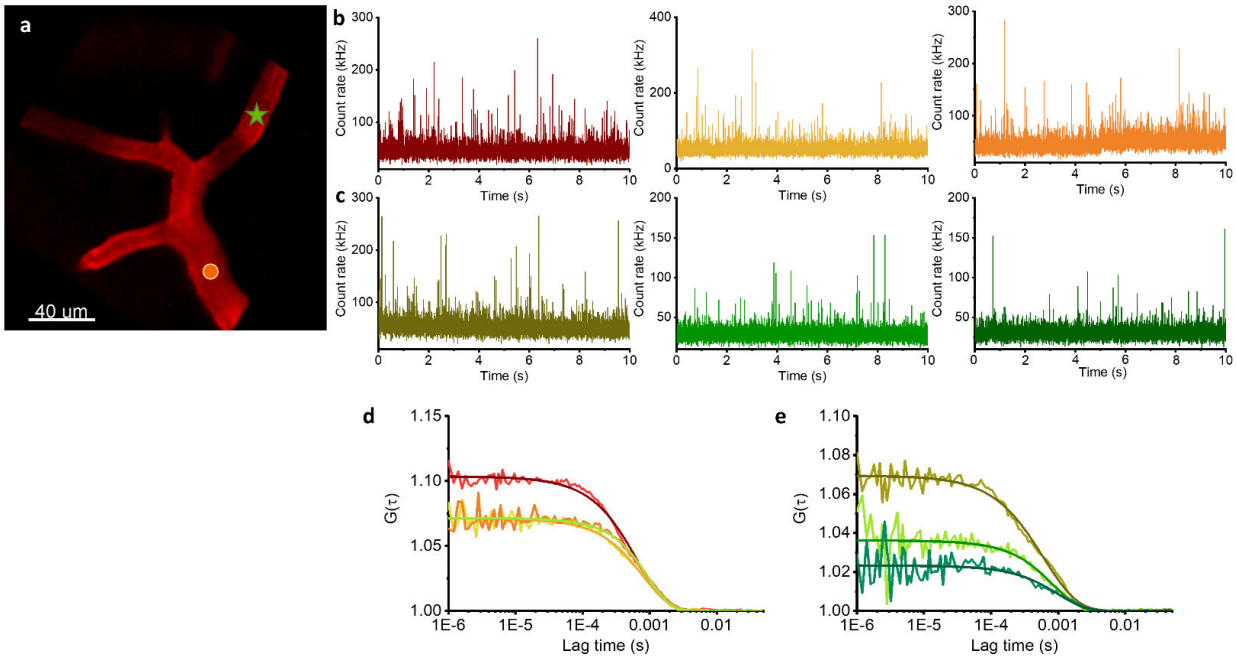

Figure S9: Dynamic *in vivo* blood flow measurements.

a. A 2P-image indicating the two points of the FCS measurements. **b.** Fluorescence intensity time traces recorded at the different heart rates at the position marked with green star. The dark red panel is recorded at a heart rate of 410 bpm; the yellow panel is recorded at 360 bpm; the orange panel is recorded at 310 bpm. The heart rate was monitored and decreased by increasing the isoflurane percentage. **c.** Fluorescence intensity time traces recorded with the different heart rates at the position marked with orange circle. Similarly, the olive panel is recorded at a heart rate of 410 bpm; the bright green is recorded at 360 bpm; the dark green panel is recorded at 310 bpm. **d** and **e.** The measured autocorrelation curves and fits from color matched time traces.

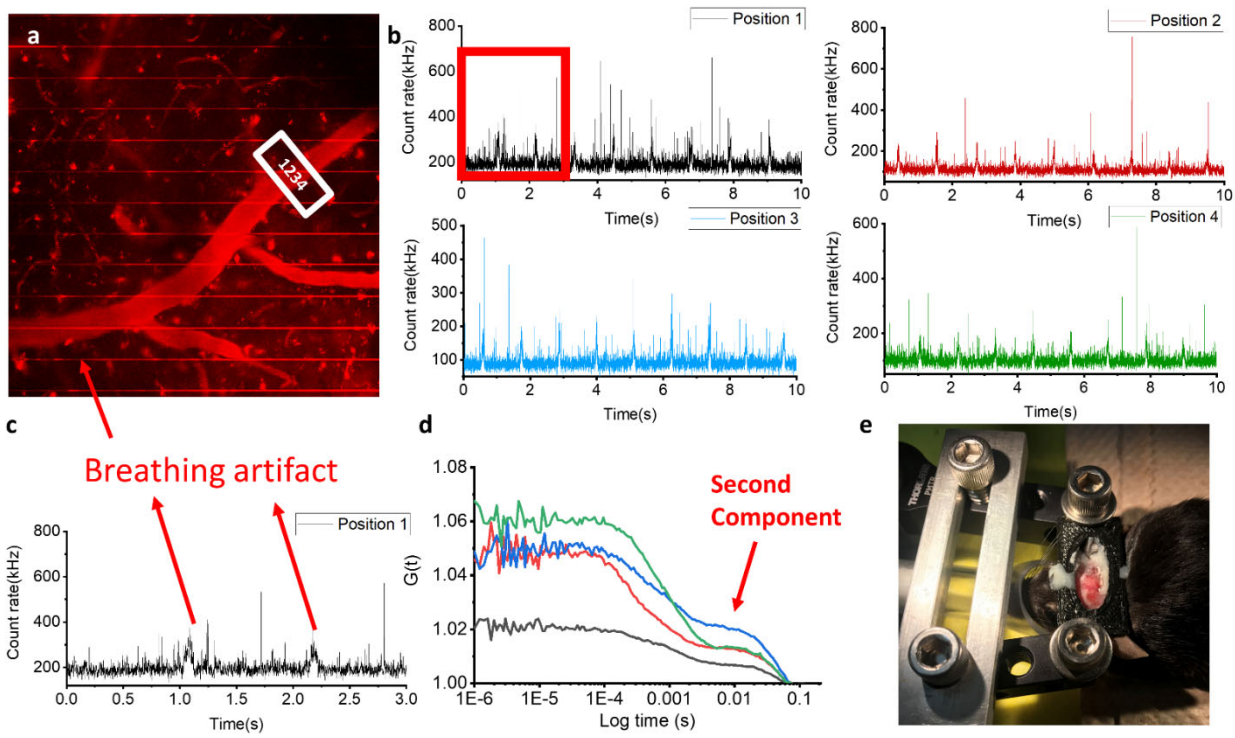

Figure S10: The effect of breath on FCS measurements and minimizing the artifacts.

a. Example image of vasculature captured showing breathing artifacts. **b.** Four representative fluorescence time traces from a cross section of one vessel. **c**. The rescaled time traces showing fluorescence fluctuations over time reveal wide bursts that are resulting from breathing artifacts in **b**. **d.** The corresponding autocorrelations identify a second longer time scale component from breathing artifacts during FCS measurements. **e.** A custom-made head restraint was used to limit the breathing motion artifacts. The restraint was mounted on the mouse head after the cranial window preparation. The edge of the skin was fixed by spreading the glue all over the skull. Dental cement was used to fasten the holder on the skull. The 3d printed holder was secured between washers onto the side bars. The 1mm thick holder has a large window in the middle, which is thick enough to stabilize the mouse head, but not to affect the working distance of the objective.

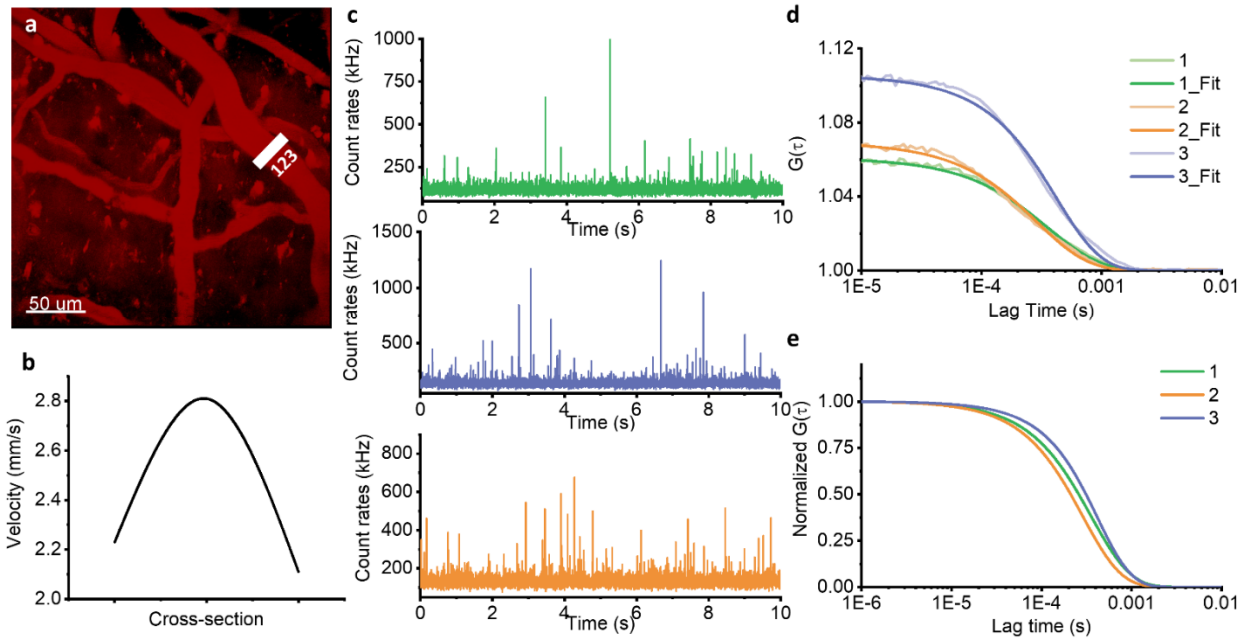

Figure S11: Blood flow measurements using Cy3-dextran 250kDa.

The vessel is imaged using Rhodamine B-dextran 500 kDa. However, the FCS measurements dye is changed to Cy3-dextran 250 kDa to of CF488-dextran 250 kDa. **a.** The 2P-image indicates the 3 points of the FCS measurements. **b** shows the relative cross section blood flow velocity profile from the marked position. **c.** Fluorescence intensity time traces recorded using the three positions with Cy3-dextran 250 kDa. **d.** The measured and fitted autocorrelation curves from color matched time traces. **e.** The normalized autocorrelation curves from **d**.

1. Negwer, I.; Best, A.; Schinnerer, M.; Schäfer, O.; Capeloa, L.; Wagner, M.; Schmidt, M.; Mailänder, V.; Helm, M.; Barz, M.; Butt, H.-J.; Koynov, K., Monitoring drug nanocarriers in human blood by near-infrared fluorescence correlation spectroscopy. *Nature Communications* **2018,** *9* (1), 5306.
2. Kim, S. A.; Heinze, K. G.; Schwille, P., Fluorescence correlation spectroscopy in living cells. *Nature Methods* **2007,** *4* (11), 963-973.